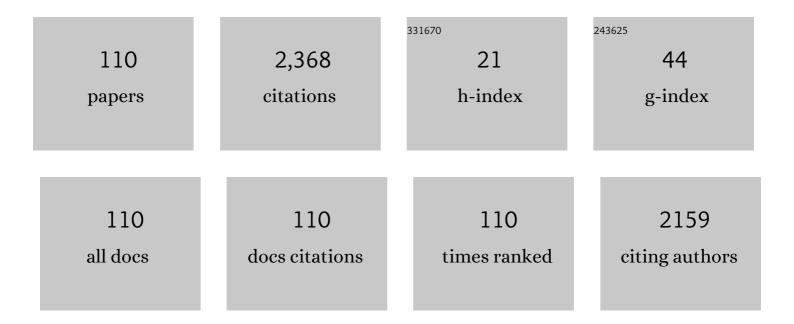
Kikuo Makita

List of Publications by Year in descending order

Source: https://exaly.com/author-pdf/3366983/publications.pdf Version: 2024-02-01



Κικιίο Μλκιτλ

#	Article	IF	CITATIONS
1	Photocatalytic generation of hydrogen by core-shell WO3/BiVO4 nanorods with ultimate water splitting efficiency. Scientific Reports, 2015, 5, 11141.	3.3	464
2	Si Nano-Photodiode with a Surface Plasmon Antenna. Japanese Journal of Applied Physics, 2005, 44, L364-L366.	1.5	300
3	Observation of a new ordered phase inAlxIn1â^'xAs alloy and relation between ordering structure and surface reconstruction during molecular-beam-epitaxial growth. Physical Review Letters, 1994, 72, 673-676.	7.8	111
4	Electrical and optical interconnection for mechanically stacked multi-junction solar cells mediated by metal nanoparticle arrays. Applied Physics Letters, 2012, 101, .	3.3	68
5	Temperature dependence of impact ionization coefficients in InP. Journal of Applied Physics, 1986, 59, 476-481.	2.5	55
6	High-speed and low-dark-current flip-chip InAlAs/InAlGaAs quaternary well superlattice APDs with 120 GHz gain-bandwidth product. IEEE Photonics Technology Letters, 1993, 5, 675-677.	2.5	48
7	Single photoelectron trapping, storage, and detection in a field effect transistor. Physical Review B, 2003, 67, .	3.2	47
8	Impact ionization rates in. IEEE Electron Device Letters, 1990, 11, 437-438.	3.9	45
9	IIIâ€V//Si multijunction solar cells with 30% efficiency using smart stack technology with Pd nanoparticle array. Progress in Photovoltaics: Research and Applications, 2020, 28, 16-24.	8.1	43
10	Palladium nanoparticle array-mediated semiconductor bonding that enables high-efficiency multi-junction solar cells. Japanese Journal of Applied Physics, 2016, 55, 025001.	1.5	37
11	Planar-structure InP/InGaAsP/InGaAs avalanche photodiodes with preferential lateral extended guard ring for 1.0-1.6 mu m wavelength optical communication use. Journal of Lightwave Technology, 1988, 6, 1643-1655.	4.6	36
12	Reliability of mesa-structure InAlGaAs-InAlAs superlattice avalanche photodiodes. IEEE Photonics Technology Letters, 1996, 8, 824-826.	2.5	35
13	High-efficiency III–V//Si tandem solar cells enabled by the Pd nanoparticle array-mediated "smart stack― approach. Applied Physics Express, 2017, 10, 072301.	2.4	34
14	Monolithically integrated In0.53Ga0.47As-PIN/InP-MISFET photoreceiver. Electronics Letters, 1984, 20, 314.	1.0	32
15	Gain-bandwidth product analysis of InAlGaAs-InAlAs superlattice avalanche photodiodes. IEEE Photonics Technology Letters, 1996, 8, 269-271.	2.5	29
16	High-speed, high-reliability planar-structure superlattice avalanche photodiodes for 10-Gb/s optical receivers. Journal of Lightwave Technology, 2000, 18, 2200-2207.	4.6	29
17	High-speed planar-structure Inp/InGaAsP/InGaAs avalanche photodiode grown by VPE. Electronics Letters, 1984, 20, 653.	1.0	28
18	Tandem photovoltaic–photoelectrochemical GaAs/InGaAsP–WO ₃ /BiVO ₄ device for solar hydrogen generation. Japanese Journal of Applied Physics, 2016, 55, 04ES01.	1.5	28

#	Article	IF	CITATIONS
19	40â€Gbit/s waveguide avalanche photodiode with p-type absorption layer and thin InAlAs multiplication layer. Electronics Letters, 2007, 43, 476.	1.0	25
20	10-gigabit-per-second high-sensitivity and wide-dynamic-range APD-HEMT optical receiver. IEEE Photonics Technology Letters, 1996, 8, 1232-1234.	2.5	24
21	High-speed, high-power and high-efficiency photodiodes with evanescently coupled graded-index waveguide. Electronics Letters, 2000, 36, 972.	1.0	23
22	A transceiver PIC for bidirectional optical communication fabricated by bandgap energy controlled selective MOVPE. IEEE Photonics Technology Letters, 1996, 8, 361-363.	2.5	22
23	Dark Current and Breakdown Analysis in In(Al)GaAs/InAlAs Superlattice Avalanche Photodiodes. Japanese Journal of Applied Physics, 1996, 35, 3440-3444.	1.5	22
24	InAlAs avalanche photodiodes with very thin multiplication layer of 0.1 [micro sign]m for high-speed and low-voltage-operation optical receiver. Electronics Letters, 2000, 36, 1807.	1.0	22
25	A high-sensitivity APD receiver for 10-Gb/s system applications. IEEE Photonics Technology Letters, 1996, 8, 1229-1231.	2.5	21
26	High-reliability and low-dark-current 10-Gb/s planar superlattice avalanche photodiodes. IEEE Photonics Technology Letters, 1997, 9, 1619-1621.	2.5	21
27	Composition control of Cu2ZnSnSe4-based solar cells grown by coevaporation. Thin Solid Films, 2014, 551, 27-31.	1.8	21
28	Illâ€V//Cu _{<i>x</i>} In _{1â^'<i>y</i>} Ga _{<i>y</i>} Se ₂ multijunction solar cells with 27.2% efficiency fabricated using modified smart stack technology with Pd nanoparticle array and adhesive material. Progress in Photovoltaics: Research and Applications, 2021, 29, 887-898.	8.1	21
29	Ga1â^'yInyAs/InAsxP1â^'x (y > 0.53, x > 0) pin photodiodes for long wavelength regions (λ > 2μm) grown by hydride vapour phase epitaxy. Electronics Letters, 1988, 24, 379.	1.0	21
30	High-sensitivity 10 Gbit/s optical receiver with superlattice APD. Electronics Letters, 1993, 29, 1874.	1.0	20
31	InAlGaAs impact ionization rates in bulk, superlattice, and sawtooth band structures. Applied Physics Letters, 1994, 65, 3248-3250.	3.3	20
32	Design and performance of InAlGaAs/InAlAs superlattice avalanche photodiodes. Journal of Lightwave Technology, 1997, 15, 1012-1019.	4.6	19
33	Investigation of the properties of semiconductor wafer bonding in multijunction solar cells via metal-nanoparticle arrays. Journal of Applied Physics, 2017, 122, .	2.5	19
34	High-temperature aging tests on planar structure InGaAs/InP PIN photodiodes with Ti/Pt and Ti/Au contact. Electronics Letters, 1984, 20, 654.	1.0	18
35	Selective growth of InAlAs by low pressure metalorganic vapor phase epitaxy. Journal of Crystal Growth, 1996, 162, 25-30.	1.5	18
36	Feasibility study of two-terminal tandem solar cells integrated with smart stack, areal current matching, and low concentration. Progress in Photovoltaics: Research and Applications, 2017, 25, 255-263.	8.1	18

#	Article	IF	CITATIONS
37	Improvement of Heterointerface Properties of GaAs Solar Cells Grown With InGaP Layers by Hydride Vapor-Phase Epitaxy. IEEE Journal of Photovoltaics, 2019, 9, 154-159.	2.5	18
38	Planar InP/InGaAs avalanche photodiodes with preferential lateral extended guard ring. IEEE Electron Device Letters, 1986, 7, 257-258.	3.9	17
39	Large bandgap energy control of multiple quantum wells selectively grown by low-pressure MOVPE. Journal of Crystal Growth, 1997, 170, 669-673.	1.5	17
40	InGaP/GaAs tandem solar cells fabricated using solid-source molecular beam epitaxy. Japanese Journal of Applied Physics, 2014, 53, 05FV06.	1.5	17
41	10â€Gbit/s asymmetric waveguide APD with high sensitivity of â^'30â€dBm. Electronics Letters, 2006, 42, 11	7710	15
42	Ultrafast growth of InGaP solar cells via hydride vapor phase epitaxy. Applied Physics Express, 2019, 12, 052004.	2.4	15
43	Dry etching and consequent burring regrowth of nanosize quantum wells stripes using an in situ ultrahigh vacuum multichamber system. Journal of Vacuum Science & Technology an Official Journal of the American Vacuum Society B, Microelectronics Processing and Phenomena, 1998, 16, 1.	1.6	14
44	Dual-junction GaAs solar cells and their application to smart stacked III–V//Si multijunction solar cells. Applied Physics Express, 2018, 11, 052301.	2.4	14
45	Fabrication of GaAs solar cells grown with InGaP layers by hydride vapor-phase epitaxy. Japanese Journal of Applied Physics, 2018, 57, 08RD06.	1.5	14
46	A new planar-structure InAlGaAs-InAlAs superlattice avalanche photodiode with a Ti-implanted guard-ring. IEEE Photonics Technology Letters, 1996, 8, 827-829.	2.5	13
47	Over 25-dB Dynamic Range 10-/1-Gbps Optical Burst-mode Receiver using High-power-tolerant APD. , 2009, , .		13
48	Impact of nanometer air gaps on photon recycling in mechanically stacked multi-junction solar cells. Optics Express, 2019, 27, A1.	3.4	13
49	Oxygen addition purification effect in InGaAs growth by hydride VPE. Journal of Crystal Growth, 1984, 69, 613-615.	1.5	12
50	Effects of substrate misorientation on triple-period ordering in AlInAs. Journal of Crystal Growth, 1995, 150, 533-538.	1.5	12
51	Investigation of the open-circuit voltage in mechanically stacked InGaP/GaAs//InGaAsP/InGaAs solar cells. Japanese Journal of Applied Physics, 2017, 56, 08MC01.	1.5	12
52	Photoluminescence study of InGaAs grown on InP by vapor phase epitaxy—Effects of O2injection and substrate orientation. Applied Physics Letters, 1985, 46, 1069-1071.	3.3	11
53	High efficiency and radiation resistant InGaP/GaAs//CIGS stacked solar cells for space applications. , 2016, , .		11
54	Epitaxial Lift-Off of Single-Junction GaAs Solar Cells Grown Via Hydride Vapor Phase Epitaxy. IEEE Journal of Photovoltaics, 2021, 11, 93-98.	2.5	11

#	Article	IF	CITATIONS
55	Over 20% Efficiency Mechanically Stacked Multi-Junction Solar Cells Fabricated by Advanced Bonding Using Conductive Nanoparticle Alignments. Materials Research Society Symposia Proceedings, 2013, 1538, 167-171.	0.1	10
56	Growth of InGaAsP solar cells and their application to triple-junction top cells used in smart stack multijunction solar cells. Journal of Vacuum Science and Technology B:Nanotechnology and Microelectronics, 2017, 35, .	1.2	10
57	Effect of Series Resistances on Conversion Efficiency of GaAs/Si Tandem Solar Cells With Areal Current-Matching Technique. IEEE Journal of Photovoltaics, 2018, 8, 654-660.	2.5	10
58	High Doping Performance of Sulfur and Zinc Dopants in Tunnel Diodes Using Hydride Vapor Phase Epitaxy. IEEE Journal of Photovoltaics, 2020, 10, 749-753.	2.5	10
59	Impact of loading topology and current mismatch on current–voltage curves of three-terminal tandem solar cells with interdigitated back contacts. Solar Energy Materials and Solar Cells, 2021, 221, 110901.	6.2	10
60	28.3% Efficient Ill–V Tandem Solar Cells Fabricated Using a Tripleâ€Chamber Hydride Vapor Phase Epitaxy System. Solar Rrl, 2022, 6, .	5.8	10
61	Microlens-integrated large-area InAlGaAs-InAlAs superlattice APD's for eye-safety 1.5-μm wavelength optical measurement use. IEEE Photonics Technology Letters, 1998, 10, 576-578.	2.5	9
62	Multiplication Noise Characterization of InAlAs-APD With Heterojunction. IEEE Photonics Technology Letters, 2009, 21, 1852-1854.	2.5	9
63	Enhancement of open circuit voltage in InGaAsP-inverted thin-film solar cells grown by solid-source molecular beam epitaxy. Journal of Crystal Growth, 2017, 477, 267-271.	1.5	9
64	Light absorption enhancement in thin-film GaAs solar cells with flattened light scattering substrates. Journal of Applied Physics, 2017, 122, .	2.5	9
65	Cu Nanoparticle Array-Mediated III–V/Si Integration: Application in Series-Connected Tandem Solar Cells. ACS Applied Energy Materials, 2020, 3, 3445-3453.	5.1	9
66	Integration of Si Heterojunction Solar Cells with III–V Solar Cells by the Pd Nanoparticle Array-Mediated "Smart Stack―Approach. ACS Applied Materials & Interfaces, 2022, 14, 11322-11329.	8.0	9
67	InAlGaAs Staircase Avalanche Photodiodes. Japanese Journal of Applied Physics, 1994, 33, L32-L34.	1.5	8
68	A planar slab-waveguide photodiode with a pseudowindow region in front of the waveguide. IEEE Photonics Technology Letters, 1998, 10, 255-257.	2.5	8
69	Design and Fabrication of a Waveguide Photodiode for 1.55-µm-Band Access Receivers. Japanese Journal of Applied Physics, 1999, 38, 1211-1214.	1.5	8
70	Pd-mediated mechanical stack of III–V solar cells fabricated via hydride vapor phase epitaxy. Solar Energy, 2021, 224, 142-148.	6.1	8
71	Application of polydimethylsiloxane surface texturing on III-V//Si tandem achieving more than 2 % absolute efficiency improvement. Optics Express, 2020, 28, 3895.	3.4	8
72	InGaP/GaAs dualâ€junction solar cells with AlInGaP passivation layer grown by hydride vapor phase epitaxy. Progress in Photovoltaics: Research and Applications, 2021, 29, 1285-1293.	8.1	7

#	Article	IF	CITATIONS
73	Perfect Matching Factor between a Customized Double-Junction GaAs Photovoltaic Device and an Electrolyzer for Efficient Solar Water Splitting. ACS Applied Energy Materials, 2022, 5, 8241-8253.	5.1	7
74	Doping Properties of Zinc in InAlGaAs Grown by Low-Pressure Metal-Organic Vapor-Phase Epitaxy. Japanese Journal of Applied Physics, 1994, 33, 3359-3361.	1.5	6
75	High-frequency response limitation of high-performance InAlGaAs/InAlAs superlattice avalanche photodiodes. Electronics Letters, 1999, 35, 2228.	1.0	6
76	Theoretical and Experimental Study on Waveguide Avalanche Photodiodes With an Undepleted Absorption Layer for 25-Gb/s Operation. Journal of Lightwave Technology, 2011, 29, 153-161.	4.6	6
77	Investigation of InGaP/(In)AlGaAs/GaAs triple-junction top cells for smart stacked multijunction solar cells grown using molecular beam epitaxy. Japanese Journal of Applied Physics, 2015, 54, 08KE02.	1.5	6
78	Multiple epitaxial lift-off of stacked GaAs solar cells for low-cost photovoltaic applications. Japanese Journal of Applied Physics, 2020, 59, 052003.	1.5	6
79	Gas source molecular beam epitaxy grown InGaAsP/InGaAlAs multi-quantum well structures with wide range continuum band-offset control. Journal of Crystal Growth, 1995, 150, 579-584.	1.5	5
80	High-crystallinity MOVPE-grown sawtooth-bandgap In1 â^' x â^' yGaxAlyAs for use in staircase avalanche photodiodes. Journal of Crystal Growth, 1997, 180, 9-14.	1.5	5
81	Highly efficient and reliable mechanically stacked multi-junction solar cells using advanced bonding method with conductive nanoparticle alignments. , 2014, , .		5
82	MBE-grown InGaAsP solar cells with 1.0 eV bandgap on InP(001) substrates for application to multijunction solar cells. Japanese Journal of Applied Physics, 2015, 54, 08KE10.	1.5	5
83	Evaluation of GaAs solar cells grown under different conditions via hydride vapor phase epitaxy. Journal of Crystal Growth, 2020, 537, 125600.	1.5	5
84	GaAs//CuIn _{1â^'y} Ga _y Se ₂ Three-Junction Solar Cells With 28.06% Efficiency Fabricated Using a Bonding Technique Involving Pd Nanoparticles and an Adhesive. IEEE Journal of Photovoltaics, 2022, 12, 639-645.	2.5	5
85	Band Offset Dependance on Impact Ionization Rates in InAlGaAs Staircase Avalanche Photodiodes. Japanese Journal of Applied Physics, 1995, 34, L1048-L1050.	1.5	4
86	Superlattice avalanche photodiodes for optical communications. Optical and Quantum Electronics, 1998, 30, 219-238.	3.3	4
87	Cross-sectional scanning tunneling microscopy observation of atomic arrangement in triple period-A type ordered AllnAs alloy. Applied Surface Science, 2005, 241, 9-13.	6.1	4
88	Reduction of bonding resistance of two-terminal III–V/Si tandem solar cells fabricated using smart-stack technology. Japanese Journal of Applied Physics, 2017, 56, 122302.	1.5	4
89	Spectral response measurements of each subcell in monolithic triple-junction GaAs photovoltaic devices. Applied Physics Express, 2019, 12, 102015.	2.4	4
90	Crystallinity and interdiffusion in InP/InGaAs quantum wells grown by Hydride VPE. Superlattices and Microstructures, 1988, 4, 101-105.	3.1	3

#	Article	IF	CITATIONS
91	InAIGaAs selective MOVPE growth with bandgap energy shift. Journal of Electronic Materials, 1996, 25, 375-378.	2.2	3
92	Extremely compact (0.3â€cm3) 40â€Cbitâ^•s optical receiver module with ease-of-use receptacle interface and feedthrough launcher. Electronics Letters, 2004, 40, 557.	1.0	3
93	Analysis of subcell open-circuit voltages of InGaP/GaAs dual-junction solar cells fabricated using hydride vapor phase epitaxy. Japanese Journal of Applied Physics, 2020, 59, SGGF02.	1.5	3
94	Recent Advances in Ultra-High-Speed Waveguide Photodiodes for Optical Communication Systems. IEICE Transactions on Electronics, 2009, E92-C, 922-928.	0.6	3
95	GaAs pin-photodiodes with an AlGaInP window layer for use in 650-nm wavelength GI-POF data links. IEEE Photonics Technology Letters, 1996, 8, 833-835.	2.5	2
96	Dual Evanescently Coupled Waveguide Photodiodes for Ultra-high Bit Rate DPSK/DQPSK systems. Conference Proceedings - Lasers and Electro-Optics Society Annual Meeting-LEOS, 2007, , .	0.0	2
97	MBE-grown InGaP/GaAs/InGaAsP triple junction solar cells fabricated by advanced bonding technique. , 2014, , .		2
98	InAlGaAs selective MOVPE growth with bandgap energy shift. , 0, , .		1
99	Wideband and high-efficiency AllnAs/GalnAs waveguide photodetectors for 40-Gbps receivers. , 2002, , .		1
100	Robust 40-Gb/s evanescently coupled waveguide photodiode with high efficiency for use in dual wavelengths: 1310 and 1550-nm. , 2004, 5280, 554.		1
101	40-Gbps high-sensitive waveguide photodetectors. , 2005, , .		1
102	43-Gb/s differential receiver module for RZ-DPSK. , 2008, , .		1
103	Effects of substrate misorientation on triple-period ordering in AllnAs. Journal of Crystal Growth, 1995, 150, 533-538.	1.5	1
104	Design and fabrication of a waveguide photodiode for $1.55 \cdot \hat{l}$ 4m band access receivers. , 0, , .		0
105	High-speed and high-efficiency AlInAs/GaInAs waveguide photodetectors for use in 40-Gbps applications. , 2002, , .		0
106	Development and applications of a Si nanophotodiode with a surface plasmon antenna. , 2006, , .		0
107	Dual Evanescently Coupled Waveguide Photodiodes with High Reliability for over 40-Gbps Optical Communication Systems. IEICE Transactions on Electronics, 2010, E93-C, 1655-1661.	0.6	0
108	Analytical Model for Obtaining the Ionization Rate Ratio of Mesa InAlAs Avalanche Photodiodes. Japanese Journal of Applied Physics, 2010, 49, 054302.	1.5	0

#	Article	IF	CITATIONS
109	Broadband Reflectance Reduction for Wafer Bonded III-V//Si tandem Cell Using Polydimethylsiloxane -Replicated Surface Texturing. , 2018, , .		0
110	Gas source molecular beam epitaxy grown InGaAsP/InGaAlAs multi-quantum well structures with wide range continuum band-offset control. Journal of Crystal Growth, 1995, 150, 579-584.	1.5	0